Segmentation in the Canine Head

A Thesis Submitted to the
College of Graduate and Postdoctoral Studies
In Partial Fulfillment of the Requirements
For the Degree of Master of Science
In the Small Animal Clinical Sciences
University of Saskatchewan
Saskatoon

By

Eric Walther, DVM

PERMISSION TO USE

In presenting this thesis in partial fulfillment of the requirements for a Postgraduate degree from the University of Saskatchewan, I agree that the Libraries of this University may make it freely available for inspection. I further agree that permission for copying of this thesis in any manner, in whole or in part, for scholarly purposes may be granted by the professor or professors who supervised my thesis work or, in their absence, by the Head of the Department or the Dean of the College in which my thesis work was done. It is understood that any copying or publication or use of this thesis or parts thereof for financial gain shall not be allowed without my written permission. It is also understood that due recognition shall be given to me and to the University of Saskatchewan in any scholarly use which may be made of any material in my thesis.

Requests for permission to copy or to make other use of material in this thesis in whole or part should be addressed to:

Head of Department of Small Animal Clinical Sciences

University of Saskatchewan

52 Campus Drive

Saskatoon, Saskatchewan, S7N 5B4

OR

Dean

College of Graduate and Postdoctoral Studies

University of Saskatchewan

116 Thorvaldson Building, 110 Science Place

Saskatoon, Saskatchewan S7N 5C9 Canada

ABSTRACT

This thesis is comprised of two research projects. Both projects focus on the contouring phase of the computerized treatment planning process for radiation therapy. Lack of agreement between human radiation oncologists on the exact location of normal tissues and tumor is well-established; this graduate work explored the lack of agreement between veterinary radiation oncologists, the impact of lack of agreement on delivered dose, and whether agreement could be improved using a new contouring method.

The goal of the first study was to quantify the dosimetric impact of the lack of interobserver agreement on GTV delineation for canine meningioma. A previously reported population of 13 dogs with GTVs contoured on CT alone and on registered CT-MR by 18 radiation oncologists was used. The 'true' GTV was generated for each dog using a STAPLE algorithm, and 'true' brain, defined as whole brain minus true GTV. Treatment plans were generated for each dog-observer combination, using criteria applied to the observer's GTV and brain contours. The mean percent coverage of true GTV by prescribed dose was higher for CT-MR plans than for CT plans (mean difference 5.9%, 95% CI 3.7 to 8.0, $p < 0.001$). There was no difference in mean volume of true brain receiving ≥ 24 Gy and in maximum true brain dose between CT plans and CT-MR plans ($p \geq 0.198$). CT-MR plans were more likely to pass criteria for true GTV and brain than CT plans (OR 1.75, 95% CI 1.02 to 3.01, $p = 0.044$). A significant dosimetric impact was demonstrated when GTV contouring was performed on CT alone compared to CT-MR.

The second study researched a new method for contouring the OP with only CT imaging. Expert consensus OP contours were delineated on registered CT and MRI for eight dogs. Twenty-one ROs contoured the OP on CT using their preferred method, and again after being

provided with an training material demonstrating contouring on the optic plane. The DSC was used to assess contour accuracy. The median DSC before training was 0.31 (5^{th} and 95^{th} percentile, 0.06, 0.48) and the median DSC after training was 0.41 (0.18, 0.53). The mean DSC was higher after training than before training (mean difference = 0.10, 95% CI 0.08 to 0.12, p <0.001) on average across all observers and patients. Use of MRI for OP contouring is expected to provide the highest accuracy, but if CT is used, the use of an optic plane should improve accuracy.

ACKNOWLEDGEMENTS

I would like to acknowledge Dr. Rick Chetney for taking the time to introduce me to radiation oncology. Without that initial introduction, my veterinary career would have very likely gone down a different path.

I would also like to thank Dr. Michael Deveau, who has continued to be supportive of me long after completing a radiation oncology internship at Texas A&M University. His patience and willingness to answer all my questions provided me with an excellent starting foundation for a career in radiation oncology.

I would especially like to thank Dr. Monique Mayer for being my supervisor for the past two years, supervising my research and teaching me many of the radiation therapy concepts I will eventually put into practice. She is an excellent instructor and her guidance in my research was invaluable.

Thank you to my committee members, Dr. Monique Mayer, Dr. Valerie MacDonald, Dr. Michael Deveau, Dr. Neal Mauldin, and Dr. Eric Boshoven for their assistance and guidance through this program. I would also like to thank PetCure Oncology for providing the funding for this research and my residency program.

TABLE OF CONTENTS

LIST OF TABLES

LIST OF FIGURES

LIST OF ABBREVIATIONS

CI: conformity index

CT: computed tomography

CTV: clinical target volume

DICOM: Digital Imaging and Communications

DSC: Dice Similarity Coefficient

GTV: gross tumor volume

MR: magnetic resonance

MRI: magnetic resonance imaging

OAR: organ at risk

OP: optic pathway

OR: odds ratio

PTV: planning target volume

SRT: Stereotactic Radiation Therapy

STAPLE: Simultaneous Truth and Performance Level Estimation

TPS: treatment planning system

VMAT: Volumetric Modulated Arc Therapy

1. CHAPTER ONE: INTRODUCTION

Computerized inverse treatment planning has revolutionized external beam radiation therapy delivery, enabling superior dose targeting over manually created plans. Superior dose targeting has resulted in better tumor dose coverage while reducing dose to normal tissues. Resulting outcomes from treatment planning systems (TPS) tend to have better tumor control and reduced acute and late side effects. The typical workflow to support a TPS in veterinary medicine begins with acquisition of CT simulation, followed by contouring of target volumes and critical structures, and ending with dosimetric calculations and treatment delivery. Each step in the process must be performed with accuracy to ensure that the patient receives the prescribed dose of radiation and has the best possible outcome.

Systematic error, or errors that occur in the treatment planning process and are propagated through the entire treatment process, can occur in the CT simulation phase, contouring phase, or the planning phase. The CT simulation can introduce systematic error from selection of an inappropriately large slice thickness. Due to slice averaging, as slice thickness increases, the dimensions of objects imaged become elongated in the cranial to caudal direction, which could result in contours encompassing tissues that were not intended. Error can be introduced in the contouring phase additionally by inaccurate target selection, which would include the gross tumor volume (GTV), or the region of tumor visible on imaging, the clinical target volume (CTV), or the presumed disease extension beyond what is visible on imaging, and the planning target volume (PTV), which is the expansion on the GTV (or CTV if present) to account for setup error. This form of error is introduced by selection resulting from inadequately visible tumors and/or inaccurate assessment of tumor volume and invasiveness. In the treatment planning phase,

systematic error would be introduced if the plan was not fully optimized to properly treat the target area while protecting normal tissues and OARs.

It is the systematic error in the contouring phase that this thesis intends to quantify and look for ways to improve. The first chapter adds to the current body of work recommending multimodal imaging when treating canine brain tumors by examining the dosimetric impact of contouring variations introduced by either CT only or CT-MRI based contouring. In the second chapter, accuracy of current CT only canine optic nerve contouring practices is investigated and compared to a new proposed method utilizing a dorsal-oblique plane to better visualize the optic nerves.

2. CHAPTER TWO: Use of CT and MR imaging in radiation therapy planning of imaging-diagnosed canine intracranial meningioma achieves better tumor coverage than CT alone

Authors: Eric Walther, Simon Warfield, Afshin Akbarzadeh, Karen Davis, Narinder Sidhu, Quinn Matthews, Michael Deveau, Neal Mauldin, Sarah Parker, Monique Mayer

2.1 Abstract

The aim of this study was to quantify the dosimetric impact of the lack of interobserver agreement on GTV delineation for canine meningioma. This study used a previously reported population of 13 dogs with GTVs contoured on CT alone and on registered CT-MR by 18 radiation oncologists. The 'true' GTV was generated for each dog using a STAPLE algorithm, and 'true' brain was defined as whole brain minus true GTV. Treatment plans were generated for each dog and observer combination, using criteria applied to the observer's GTV and brain contours. Plans were then categorized as a pass (met all planning criteria for true GTV and brain) or fail. A mixed-effects linear regression was performed to examine differences in metrics between CT and CT-MR plans, and mixed-effects logistic regression was performed to examine differences in percentages of pass/fail between CT and CT-MRI plans. The mean percent coverage of true GTV by prescribed dose was higher for CT-MR plans than for CT plans (mean difference 5.9%, 95% CI 3.7 to 8.0, $p < 0.001$). There was no difference in mean volume of true brain receiving ≥ 24 Gy and in maximum true brain dose between CT plans and CT-MR plans ($p \geq 0.198$). CT-MR plans were significantly more likely to pass criteria for true GTV and brain than CT plans (OR 1.75, 95% CI 1.02 to 3.01, $p = 0.044$). This study demonstrated significant dosimetric impact when GTV contouring was performed on CT alone compared to CT-MR.

2.2 Introduction

Meningioma is the most commonly diagnosed primary intracranial tumor in the dog[1,2] and it provides unique challenges to the veterinary radiation oncologist. As a space occupying mass sharing an enclosed area with the brain, accurate tumor delineation is critical for both ensuring adequate tumor control as well as minimizing complications to normal brain tissue and other nearby critical structures. Computed tomography (CT) is utilized by veterinary radiation therapy inverse treatment planning systems (TPSs). The ability to translate tissue attenuation from CT images to tissue density TPSs to account for tissue heterogeneity in radiation dose calculations.[3] While CT is recognized for superior image quality of bony lesions[4], the soft-tissue resolution of the tumor, brain, and surrounding tissues is inferior to magnetic resonance imaging (MRI).[5] For this reason, MRI has been recommended as an additional imaging modality.[6] The MRI can be registered with the CT within the treatment planning system and enable the radiation oncologist to better demarcate gross tumor volume (GTV) as well as organs at risk (OAR). For veterinary patients, MRI is not always performed prior to radiation planning to treat intracranial meningioma.[7,8,9] Possible reasons for not obtaining MRI include owner finances, lack of availability, or not recommended.

A human study that investigated interobserver agreement of brain tumor volume delineation on CT compared to CT registered with MRI (CT-MRI) in which nine physicians contoured five inoperable brain tumors found no reduction in interobserver variability.[10] The study used a 5 mm slice thickness and was therefore subject to a volumetric distortion not experienced with the current standard of 1 to 2 mm slice thickness.[11] A more recent study looked at interobserver variability between veterinary radiation oncologists when contouring canine intracranial meningioma. The study evaluated tumors contoured with CT alone as well as tumors

contoured with CT-MRI. A statistically significant improvement in interobserver variability was observed with CT-MRI. However, dosimetric impact of the interobserver variability was not evaluated.[12] While the study established that interobserver agreement is improved when MRI is incorporated into radiation treatment planning, it remains unclear if this improvement translates to a corresponding improvement in the dosimetry profile for radiation plans generated based on CT-MRI contouring. Although there have been studies of human patients that investigated the dosimetric impact of interobserver variability,[13,14,15] this is the first study to compare dosimetric impact of interobserver variability comparing CT to CT-MRI against a gold standard or 'true' tumor volume for canine meningioma.

We hypothesized that a reduction in interobserver variability would correspond to an improved dosimetry profile. Therefore, the aim of the current study was to quantify the dosimetric impact of the previously described lack of interobserver agreement, and to compare this dosimetric impact between treatment plans based on CT contours and those based on CT-MRI contours.

2.3 Materials and Methods

This study examines the dosimetric impact of interobserver variability in GTV definition; the interobserver agreement on GTV for the same population of patients and observers has been previously reported.[12] The patient and observer populations, imaging acquisition, and GTV delineation process are fully described in the previous study,[12] and summarized here. To study dosimetric impact, treatment plans were generated for each patient using planning criteria based on GTV and brain contours for each observer, and then the metrics for 'true' GTV and brain contours were examined.

Thirteen dogs diagnosed with a solitary intracranial meningioma based on both CT and MR imaging were included in the study. The CT and MR were acquired under the same general anesthesia and were performed between January 2014 and June 2017. All dogs were immobilized for imaging using a vacuum fixation cushion (SecureVac, Bionix Radiation Therapy, Toledo, OH), a thermoplastic neck cushion (Klarity Moldable AccuCushion, Klarity Medical Products, Newark, OH) and a custom acrylic maxillary plate with a thermoplastic bite block (EZ Bolus Thermoplastic Pellets, Klarity Medical Products, Newark, OH). A thermoplastic head mask covered the head (Green Profile Frame Extended Head Mask, Klarity Medical Products, Newark, OH) and was attached, along with the maxillary plate, to an acrylic baseplate (Klarity MultiFix AIO Baseplate, Klarity Medical Products, Newark, OH). A 16-slice CT scanner (Acquilion 16, Toshiba America Medical Systems, Tustin, CA) was used to acquire images for contouring. Scanning parameters included 100-120 kVp, 300 mA, tube rotation time 0.5 s, and 512 x 512 matrix dimensions. Iohexol (Omnipaque, 350 mgI/ml, GE Healthcare, Chicago, IL) at 2 mL/kg was administered intravenously three minutes prior to acquisition of post-contrast images. Reconstruction algorithms included soft tissue and bone window levels at a slice thickness of 2 mm. MRI acquisition was performed using a 1.5 Tesla scanner (Siemens Symphony, Siemens, Oakville, ON, Canada). Slice thickness was 2 mm with no interslice gap. Image sets obtained included pre and postcontrast T1-weighted (TR 391-760 ms, TE 11-13 ms) and T2-weighted (TR 4620 – 9000 ms, TE 88 – 138 ms), all acquired in the transverse plane. Gadoversetamide (Optimark,0.5 mmol/ml, Mallinckrodt, St. Louis, MO) at 0.2 mL/kg was administered immediately prior to acquisition of postcontrast images. Registered CT and MRI DICOM image sets were uploaded to a web-based contouring software platform (EduCase, RadOnc eLearning Center, Jackson, WY) and made available to study observers.

Eighteen board-certified veterinary radiation oncologists first contoured the GTV based on pre- and post-contrast CT images, and then, following an eight-week interval, contoured the GTV on registered pre- and post-contrast CT and pre- and post-contrast T1 and T2 MRI.

2.3.1 STAPLE Generation

To determine the potential dosimetric impact of contouring variations on clinical outcome, the true tumor volume and location was calculated for each patient (for both CT based GTV and CT-MRI based GTV) by (S.W.) and (A.A.) using a simultaneous truth and performance level estimation (STAPLE) algorithm.[16] The STAPLE algorithm utilizes multiple expert contours to calculate a best estimate of the true GTV.

For each patient, the contours of regions in each image were labelled and stored in a digital imaging and communications in medicine (DICOM) structure set file, representing the GTV contour in every two-dimensional (2D) slice. Each contour was read using a DICOM software toolkit (DCMTK, https://github.com/DCMTK/dcmtk). Each 2D polygon was scanline rendered into an image with the same geometry as the original acquisition, with voxels inside the polygon rendered as foreground and voxels outside the polygon rendered as background. This created a three-dimensional binary image representing the labelled region of interest.
The STAPLE algorithm was then used to estimate a consensus reference standard GTV segmentation from each of the 18 available binary images (18 observers) for each patient. All voxels that were labelled the same in all eighteen images were set to the value indicated in each segmentation. The reference standard estimates of the value of the voxels where there was some disagreement across segmentations was inferred via Expectation-Maximization with each segmentation characterized by a sensitivity and specificity, as previously described.[16] The contour of the region with maximum likelihood of being foreground was extracted and written in a DICOM structure set file.

2.3.2 Radiation Planning

For each of the 13 patients, radiation plans were created for the true GTV contours (STAPLE CT GTV, STAPLE CT-MR GTV) and for each of the 36 observer GTV contours (18 CT based GTV contours and 18 CT-MR based GTV contours) using treatment planning software (Eclipse versions 13.6, Varian Medical Systems, Palo Alto, CA). Normal tissue contours were created for whole brain using automatic segmentation on transverse CT images, and for optic pathway (left and right optic nerve, optic chiasm) using manual segmentation on registered CT and MR images in the transverse plane. Normal brain was defined as whole brain minus GTV, and true normal brain was defined as whole brain minus the STAPLE GTV.

A prescription of a total dose of 24 Gy administered in three consecutive daily fractions was used for all plans. An SRT treatment plan was selected for this study due to the increased importance of accurate tumor and normal brain delineation.

All plans were created by inverse planning using a volume modulated arc therapy (VMAT) technique. The CTV and PTV were both set to 0 mm. Planning criteria included a minimum 99% coverage of the GTV with the prescription dose (98% was allowed if needed to satisfy normal brain constraints), a maximum of 1.1 cm^3 of normal brain tissue receiving 24 Gy or higher,[7] a maximum point dose (defined as 0.035 cm^3)[17] to the brain of 30 Gy, a maximum point dose of 17.4 Gy to the optic pathway and no more than 0.2 cm^3 of the optic pathway to receive 15.3 Gy or higher[17].

All radiation plans were created by one of two radiation therapists with experience in veterinary radiation planning, or a veterinary radiation oncology resident (E.W.). All plans were reviewed and approved by a board-certified veterinary radiation oncologist (M.M.).

2.3.3 Treatment Plan Metrics

Dose volume histogram (DVH) data was downloaded from the treatment planning system into a database (Microsoft Access for Microsoft 365 version 2105, Microsoft Corp., Redmond, WA) that was then parsed programmatically (Microsoft Visual Basic for Applications version 1109, Microsoft Corp., Redmond, WA) to obtain the following metrics for each plan: percent true GTV coverage by the prescription dose, true brain volume receiving 24 Gy or higher, maximum point dose to true brain, and Paddick conformity index (CI).

Paddick CI is a measure of radiation treatment plan conformity with a value ranging from 0 (no conformity) to 1 (perfect conformity). The Paddick CI was calculated by the following formula: $\frac{TV_{PIV}{}^2}{TV \; x \; PIV}$ where *TV* is the target volume, *PIV* is the prescription isodose volume, and TV_{PIV} is the volume of the target volume covered by the prescription isodose volume.[18] Another metric considered was the Radiation Therapy Oncology Group conformity index that compares the prescription isodose volume to the target volume with no accounting for geometric overlap.[19] The Paddick CI was selected because it does account for geometric overlap.
Treatment plans were categorized as a pass (met all planning criteria for true GTV and true brain) or fail (did not meet one or more criteria). Plans were categorized as pass or fail using two sets of criteria for true GTV dose coverage; a minimum 98% coverage of the true GTV with the prescription dose (the dose coverage criterion used in planning) and a minimum 95% coverage of the true GTV with the prescription dose.

2.3.4 Statistical Analysis

For each plan, the median, range, and 5th and 95th percentiles were calculated for percent of true GTV covered by the prescribed dose, volume of true brain receiving 24 Gy or more,

maximum point dose to true brain and optic pathway, volume of the optic pathway receiving 15.3 Gy or higher and Paddick CI.

A mixed-effects linear regression that accounted for repeated measures on patients and by observers was performed to examine differences in percent of the true GTV covered by the prescribed dose, volume of true brain ≥ 24 Gy, maximum point dose to true brain and Paddick CI, between CT and CT-MRI imaging-based plans.

Mixed-effects logistic regression was performed to examine differences in percentages of pass/fail treatment plans between CT and CT-MRI imaging-based plans.

P-values ≤ 0.05 were considered significant. Data analysis was designed with support from an analytic epidemiologist (S.P.). All analysis were completed with commercially available software (STATA/SE version 17 for Windows, StataCorp, College Station, TX).

2.4 Results

The median age of the 13 dogs was 9.8 years (range: 5.3 to 13.0 years), the median weight was 19.5 kg (range: 5.6 to 44.0 kg), and there were 8 neutered males and 5 spayed females. Breeds consisted of mixed (n = 6), Soft-Coated Wheaten Terrier (n = 3), Boston Terrier (n = 1), Miniature Schnauzer (n = 1), Flat-Coated Retriever (n = 1), and German Shepherd (n = 1). Tumor locations include cerebellopontomedullary angle (n = 4), basilar (n = 4), olfactory (n = 3), and cerebral convexity (n = 1). Four of the dogs had histologically confirmed meningioma on postmortem analysis.

There were some instances where a slice within a patient's GTV volume was not contoured by an observer, and these GTV volumes (n = 11) were excluded from the study.

Accounting for these excluded observer GTVs, 483 SRT plans were developed for all observer and STAPLE generated GTV and brain contours. Planning criteria for GTV and brain were met for all plans. The optic pathway was near the GTV in four dogs, and of these dogs, three dogs met the planning criteria for the optic pathway. In one dog, the tumor was located next to the optic chiasm with many observer GTV contours overlapping the chiasm. For this dog, it was not possible to meet the optic constraints in five observer CT plans, the CT-MRI STAPLE plan, and eighteen of the participant CT-MRI plans for a total of 24/38 (63%) plans.

Figure 2.1 shows dose volume histograms (DVHs) in a single dog for all observer GTV and brain contours based on CT imaging only, and on CT-MR imaging. The DVH lines for plans created for contours drawn with co-registered MR show a narrower spread between observers than the plans created for contours drawn with CT only.

2.4.1 Dosimetric Impact of Imaging on True GTV and True Brain Dose

Median true GTV volume (based on STAPLE algorithm calculations) was 2.19 cm^3 (range: 1.29 to 6.06 cm^3) for CT and 3.07 cm^3 (range: 1.66 to 8.25 cm^3) for CT-MRI. Median true normal brain volume (also based on STAPLE algorithm calculations) was 80.7 cm^3 (range: 62.8 to 103.3 cm^3) for CT and 80.2 cm^3 (range: 62.5 to 103.6 cm^3) for CT-MRI.

Descriptive statistics for true GTV coverage, true brain dose, maximum point dose to true normal brain, and Paddick conformity index are presented in Table 2.1. Scatter plots in Figure 2.2 show the percentage of true GTV and the volume of true brain receiving the prescribed dose or higher for all observer plans. There was a tighter clustering in the high GTV percent coverage, low brain volume region for the CT-MR based plans than for the CT based plans.

When dose to true GTV and true brain were considered, 15% (34/229) of plans using contouring on registered CT imaging alone were categorized as a pass (met all study planning

criteria) and 21% (49/228) of plans using contouring from CT-MRI were categorized as a pass. When the dose coverage criterion was changed to a minimum 95% coverage of the GTV with the prescription dose, 33% (76/229) of plans using contouring on registered CT alone imaging were categorized as a pass and 52% (118/228) of plans using contours from CT-MRI were categorized as a pass.

The mean percent coverage of true GTV by prescribed dose was higher for plans using contours from registered CT-MR imaging than for plans using contours from CT alone (mean difference between CT-MR and CT = 5.9%, 95% CI 3.7 to 8.0, $p < 0.001$) on average across all observers and patients. There was no difference in mean volume of true brain receiving ≥ prescribed dose and in maximum true brain point dose between plans on contours created using registered CT-MR imaging and plans using CT alone ($p = 0.523$ and $p = 0.198$, respectively). The mean Paddick CI was higher for plans using contours from registered CT-MR imaging than for plans using contours from CT alone (mean difference between CT-MR and CT = 0.05, 95% CI 0.03 to 0.07, $p < 0.001$) on average across all observers and patients.

Plans based on CT-MRI contours were more likely to pass study criteria for true GTV and true brain than plans based on contours from CT alone (OR 1.75, 95% CI 1.02 to 3.01, $p = 0.044$). Plans based on CT-MRI contours were more likely to pass study criteria than plans based on contours from CT alone when the true GTV dose criterion was changed to a minimum 95% coverage by the prescribed dose (OR 2.36, 95% CI 1.56 to 3.59, $p < 0.001$).

2.5 Discussion

This study demonstrated significant dosimetric impact results when contouring of intracranial meningioma is performed on CT images alone compared to contouring with both CT

and MR images, with a significant increase in percent GTV coverage with the prescription dose when MRI is added. Furthermore, despite a significantly increased 'true' tumor volume resulting from CT-MRI delineation, there was no significant increase in dose to normal brain tissue. While the odds of creating a radiation plan that delivers an acceptable dose to both tumor and normal brain tissue are significantly increased with CT-MRI, close to three-quarters of CT plans and one-half of CT-MRI plans would not meet acceptable criteria when applied to true tumor volume.

The results of this study suggest that with CT-MRI radiation therapy planning, increased tumor coverage is possible without increasing risk to normal tissues. Additionally, this study also suggests that the dosimetric impact of interobserver variability among veterinary radiation oncologists could result in patients not receiving optimal care. Possible solutions could include a formal resident training program for contouring and additional contouring workshops requirements required for continuing education. Studies have shown that training can be effective at reducing interobserver variability for the delineation of both target volumes and organs at risk.[20-25] Open-source software has been developed to support delineation training of human anatomy that could be adapted to veterinary species and utilized in training programs.[26]

Previous studies have shown inconsistent results with regard to contouring variability when MRI is incorporated into the treatment plan. Two human studies compared variability between CT alone and MRI alone for brain and cervical tumors and found no statistical difference,[10,14] with one noting that each modality had regions delineated that were not on the other, leading to the recommendation of contouring with CT-MRI.[10] The other study, in which three physicians contoured 18 patients undergoing radiation therapy made use of the STAPLE algorithm to compare CT and MRI contours. The MRI contours were reported to be smaller, but not statistically significant. A significant increase in GTV volume was reported in both human renal cell carcinoma and canine intracranial meningioma patients when the gross tumor was

contoured with the benefit of MRI,[12,25] with the dog study also finding a significant reduction in interobserver variability.[12] One study identified a high degree of interobserver CT-MRI contouring variability for human brain metastasis and found a related dosimetric variability with a Paddick CI range from 0.26 to 0.71.[27] This is consistent with Paddick CI range for CT-MRI plans (0.33 to 0.88) found in our study.

An interesting finding of this study was that median tumor volume was about 80 cm^3 for both the CT only contours and the CT-MRI contours, while the tumor volumes where 2.2 cm^3 on CT only and 3.1 cm^3 on CT-MRI. This result could be due to the ability of MRI to detect soft tissue involvement in bone better than CT and the broad-based bone attachment often seen with intracranial meningioma. This could also explain why the volume of brain tissue exposed to 24 Gy was not statistically significant between the CT only and CT-MRI groups.

One important limitation of this study is the inability to confirm the true extent of tumor. The STAPLE algorithm has been evaluated in a human paper that found it to be a valuable estimation tool with increasing robustness with increasing input contours. The study evaluated number of contours up to twelve[28] and it has been relied on in a number of human studies for establishment of consensus guidelines.[29-33] Another limitation is the inability to compare actual clinical impact resulting from the observer contours. It would not be possible to eliminate this, as well as the previous limitation as it would not be possible to perform a necropsy on each dog and then treat each dog with a plan created from each contoured volume. Additionally, each observer was aware that volume contoured would not be used for actual treatment, so some may not have put forth the same effort that they would if patient outcome was dependent on their contours.

This study suggests that MRI incorporation into CT based radiation therapy planning for canine intracranial meningioma improves plan dosimetry through increased GTV coverage by the prescription dose while maintaining minimal dose distribution to normal brain outside of the

GTV. While this is particularly important intracranially where a large portion of the tumor volume is often surrounded by and in contact with the brain, it could also be applied to other regions where the GTV is in close proximity to OARs, such as in the oronasal region or the spinal cord.

The current study adds to existing research having identified decreased dosimetric variation with CT-MRI contouring. Improved dosimetric coverage of canine intracranial meningioma is possible with CT-MRI SRT planning. Interobserver contouring variability in our study resulted in most plans from both CT only and CT-MRI contoured plans not meeting metrics when applied to true tumor margins. More needs to be done to decrease interobserver variability among veterinary radiation oncologists.

Table 2.1. Descriptive statistics (median, range, 5th and 95th percentiles) describing the radiation dosimetry data between treatment plans developed from contouring by 18 veterinary radiation oncologists using CT or CT-MR imaging to delineate GTVs for 13 dogs with intracranial meningioma.

	CT			**CT-MR**		
	MEDIAN	**RANGE**	**5TH, 95TH PCTL**[a]	**MEDIAN**	**RANGE**	**5TH, 95TH PCTL**
STAPLE GTV Volume (cm^3)	2.2	1.3, 6.1	1.4, 5.6	3.1	1.7, 8.2	1.8, 7.4
Normal Brain Volume[a] (cm^3)	80.7	62.8, 103.3	65.2, 97.9	80.2	62.5, 103.6	65.0, 97.6
GTV %[b]	93.4	0.1, 100	58.0, 99.9	96.6	43.8, 100	71.8, 99.9
Brain 24 Gy[c] (cm^3)	0.4	0.0, 10.0	0.0, 3.0	0.6	0.0, 8.4	0.1, 1.8
Brain Max Point Dose[d] (Gy)	25.2	23.4, 29.7	24.0, 26.9	25.3	23.6, 28.4	24.3, 26.9
Paddick CI[e]	0.63	0.0, 0.83	0.33, 0.79	0.67	0.33, 0.88	0.42, 0.83

[a]Volume of normal brain determined by total brain volume not within STAPLE tumor volume

[b]Percent of GTV covered by 100% of prescription dose (24 Gy)

[c]Normal brain volume receiving ≥ 24 Gy

[d]Maximum point dose (0.035 cm^3) to normal brain

[e]Paddick conformity index

Figure 2.1: Representative DVHs from a dog in the study. The red dotted line represents dosimetry output from the plan created on STAPLE volumes, the gray lines represent dosimetry output from plans created on the observer contours overlaid on to the STAPLE volumes. Normal brain and GTV lines are displayed in each DVH.

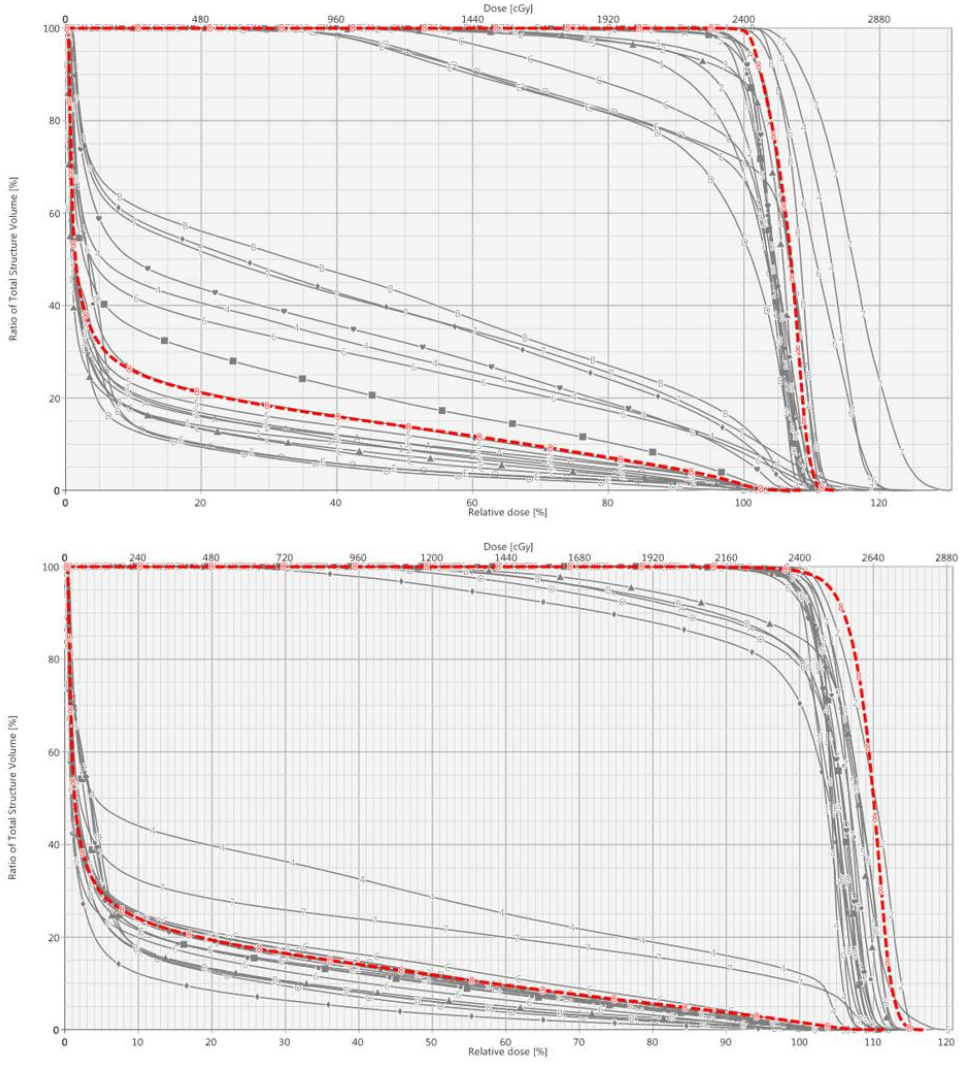

Figure 2.2 Scatter plots graphing normal brain volume receiving over 24 Gy on the y axis against tumor percent coverage on the x axis. The CT only plans are plotted on the top and the CT-MRI plans are plotted on the bottom.

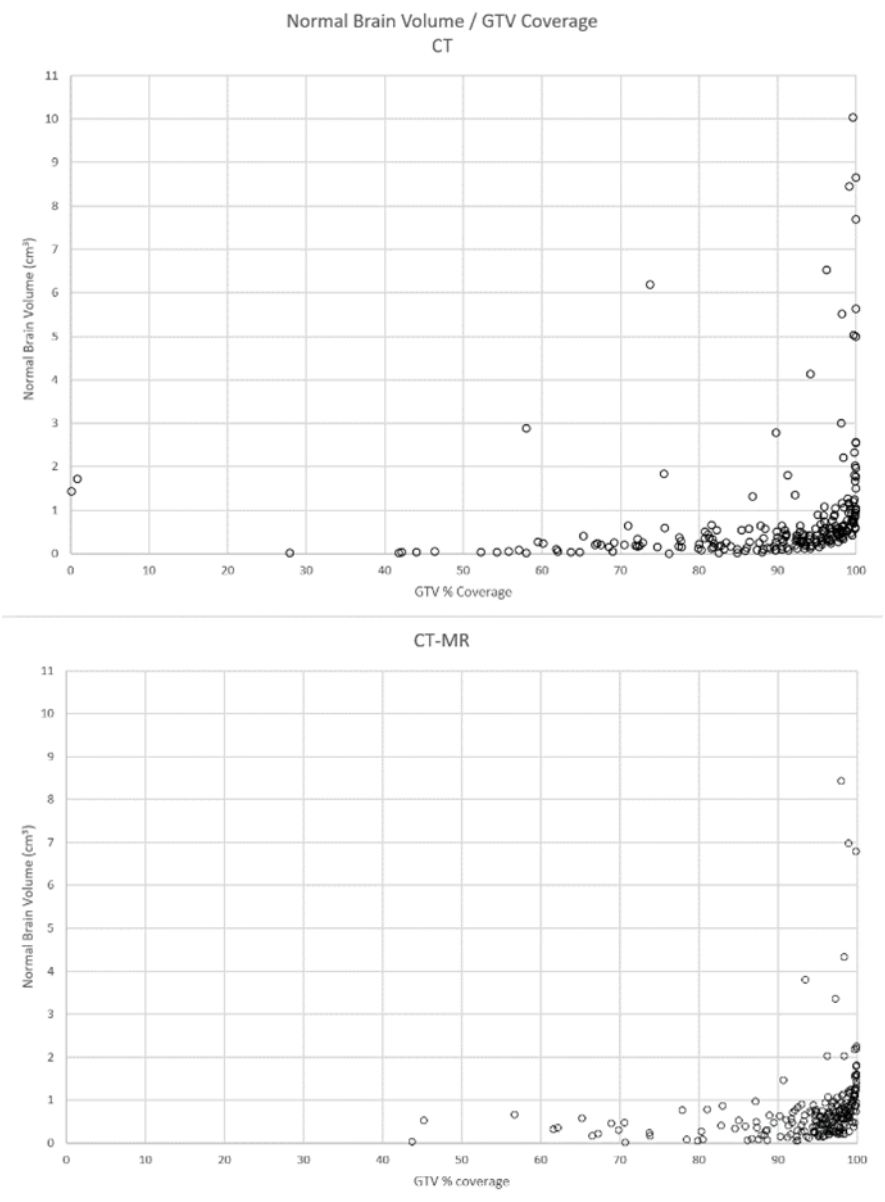

3. CHAPTER THREE: Contouring in the optic plane improves accuracy of computed tomography-based segmentation of the optic pathway

Authors: Eric Walther, Lynn Griffin, Elissa Randall, Lynne Sandmeyer, Sephanie Osinchuk, Sally Sukut, Katherine Hansen, Michele Keyerleber, Jessica Lawrence, Sarah Parker, Monique Mayer

3.1 Abstract

Optic pathway contours are often based on CT alone, however, the optic pathway is difficult to visualize with CT using standard planes. The purpose of this study was to examine accuracy of optic pathway contouring by radiation oncologists (ROs) before and after training on use of the optic plane. Expert consensus optic pathway contours were delineated on registered CT and MRI for eight dogs. Twenty-one ROs contoured the optic pathway on CT using their preferred method, and again after being provided with an atlas and video demonstrating contouring on the optic plane. The Dice similarity coefficient (DSC) was used to assess contour accuracy. A multilevel mixed model with random effects to account for repeated measures was used to examine the difference in the DSC before and after the training. The median DSC before training was 0.31 (5^{th} and 95^{th} percentile, 0.06, 0.48) and the median DSC after training was 0.41 (0.18, 0.53). The mean DSC was significantly higher after training than before training (mean difference = 0.10, 95% CI 0.08 to 0.12, $p < 0.001$) on average across all observers and patients. DSC values were comparable to those reported for segmentation of the optic chiasm and nerves in human patients (range 0.4 to 0.5). While significantly improved by the training, the accuracy of CT-based contours remained low after training. Use of MR imaging for optic pathway contouring is expected to provide the highest accuracy, but if CT is used, our study found that contouring on an optic plane will improve accuracy.

3.2 Introduction

Dose constraints for the optic pathway that may affect planning decisions by the radiation oncologist are applied during radiation treatment planning for dogs with head tumors. Radiation therapy planning for the head is often based on computed tomography (CT) alone; however, the canine optic pathway is difficult to visualize with CT imaging using standard transverse, sagittal, and dorsal planes. Optic pathway delineation is usually performed based on other anatomical landmarks when visualization of the optic pathway itself is not possible, introducing additional uncertainty in the accuracy of the contours.

With stereotactic radiation prescriptions becoming more frequently implemented in the head,[1-6] the accuracy of optic pathway contours is critical to ensure preservation of patient vision, particularly as recommended dose constraints for the optic pathway are considerably lower than many commonly used tumor dose prescriptions.[7,8,9]

Contouring guidelines could potentially improve consistency and accuracy. Unfortunately, little guidance has been published regarding optic pathway delineation for veterinary patients. Nolan, et al. published a guideline for contouring the feline optic pathway from the transverse view utilizing both CT and magnetic resonance imaging (MRI),[10] and there have been several studies identifying structures of the optic pathway in the dog.[11,12,13] However, to the authors' knowledge, there have been no studies that describe a method for contouring the canine optic pathway.

Modern contouring software allows for viewing images at any angle, enabling visualization of features commonly obscured in the standard planes. It is possible to visualize the optic nerves from the globe to the opening of the optic canals when the viewing angle is set to a dorsal oblique plane parallel to the optic nerves, henceforth referred to as the optic plane, and an

appropriate window width and level is selected. The purpose of this study was to examine accuracy of optic pathway contouring by board-certified veterinary radiation oncologists before and after training guidelines were provided for canine optic pathway contouring using an optic plane.

3.3 Materials and Methods

This study was approved by the University of Saskatchewan institutional Behavioral Ethics Review Board (BEH-2406) and the Animal Research Ethics Board (AUP-20200114). Eight client-owned dogs referred for radiation therapy were recruited for study participation. Inclusion criteria included weight > 5 kg and no disease process in the region of the optic pathway.

Each dog underwent pre-and post-contrast CT and MR imaging under the same anesthetic event; imaging was acquired between November 2020 and October 2021. All dogs were immobilized for imaging using a vacuum fixation cushion (SecureVac, Bionix Radiation Therapy, Toledo, OH), a thermoplastic neck cushion (Klarity Moldable AccuCushion, Klarity Medical Products, Newark, OH) and a custom acrylic maxillary plate with a vinyl bite block (VP MIX PUTTY, Henry Schein Inc., Melville, NY). A thermoplastic head mask covered the head (Green Profile Frame Extended Head Mask, Klarity Medical Products, Newark, OH) and was attached, along with the maxillary plate, to an acrylic baseplate (Klarity MultiFix AIO Baseplate, Klarity Medical Products, Newark, OH). A 64-slice CT scanner (Discovery MIDR, GE Medical Systems, Waukesha, WI) was used to acquire images for contouring. Scanning parameters included 120 kVp, 150 - 500 mA, tube rotation time 0.7 s, and 512 x 512 matrix dimensions. Iohexol (Omnipaque, 350 mgI/ml, GE Healthcare, Chicago, IL) at 2 mL/kg was administered

intravenously three minutes prior to acquisition of post-contrast images. Reconstruction algorithms included soft tissue and bone window levels at a slice thickness of 1.25 mm. A 1.5 Tesla MR unit (Siemens Symphony, Siemens, Oakville, ON, Canada) was used to acquire fat saturated T2-weighted (TR 3000-4000 ms, TE 75 ms) sequences in the optic plane.

The CT and MR images were registered in a treatment planning system (TPS) (Eclipse version 13.6, Varian Medical Systems, Palo Alto, CA) and the optimal window level and width for a soft tissue or full window reconstruction that distinguished the optic nerve from surrounding soft tissue were determined (Figure 2b). Consensus (gold standard) contours of the optic pathway were developed by a group of board-certified experts, including one veterinary radiation oncologist, two ophthalmologists, one radiologist, and one dual boarded radiologist and radiation oncologist. Separate contours were created for the left and right optic nerves as well as the optic chiasm.

Email invitations to participate were sent to 114 board certified veterinary radiation oncologists. Thirty-five agreed to participate in the study and each were assigned a random two-digit identifying number used to maintain confidentiality. Contouring was performed in two phases (before and after provision of an optic pathway contouring training guide). After phase one contouring was completed, a short, anonymous SurveyMonkey questionnaire was sent to all participants that completed the contours with the purpose of describing the participating population. The participants were asked five questions: how frequently they contoured the optic pathway based on CT imaging in their clinical practice, what plane(s) of CT imaging they use to contour the optic pathway and the percentage of time they use those plane(s), whether the TPS used for the study prevented them from performing any of their normal contouring practices,

what type of practice they primarily work at, and whether they had additional comments on the study (with the option to add comments).

3.3.1 Observer Contouring

Participants were supplied with remote access credentials to connect via Microsoft Remote Desktop (Microsoft Corporation, Redmond, WA) to the same treatment planning system that the consensus contours were created on. All CT image sets were anonymized and a structure set was created for each participant containing three empty structures (Optic Nerve L, Optic Nerve R, Optic Chiasm). Access to the remote system was managed through a Google Sheets document (Google, Inc., Mountain View, CA) in four- or eight-hour blocks, each separated by one hour to allow time for structure sets to be backed up and changed out in between participants. All participants independently contoured the optic pathway in all dogs using their preferred method using the supplied structures. The structure sets were associated with a post-contrast soft tissue CT reconstruction and a registered bone reconstruction was also supplied.

To reduce recall bias, participants waited at least three weeks before beginning phase two. Scheduling was done as in phase one. Participants were instructed to follow a specific contouring sequence utilizing the optic plane described in a PDF training atlas (Figure 3.1), and an optional four-minute video demonstrating the method was also provided (https://youtu.be/gvKEYLTYR08).

The training atlas instructed participants to contour using pre-set window level of 40 and a window width of 150 (corresponding to an upper gray level of 115 and a lower gray level of -35 on a soft tissue reconstruction, and then to rotate the dorsal plane view to a dorsal oblique angle coinciding with the extracranial path of the optic nerves, or the optic plane. This was achieved by

rotating the sagittal view until the hard palate of the dog was approximately 35 to 45 degrees off the vertical axis, then scrolling through the dorsal oblique (optic) plane until the maximum extracranial length of optic nerves could be visualized (Figure 3.2b).

The participants were then instructed to contour the extracranial portion of the optic nerves using the optic plane from the caudal glove to the opening of the optic canal, using a brush size of 3 to 4 mm.

After completing the extracranial contouring, the participants were directed to switch to the transverse view and use bone window to extent the contours through the optic canal to the level at which the presphenoid bone between the two optic canals begins to recede. Participants were then instructed to scroll to the next caudal slice, switch back to a window level (40) and width (150), and contour the region of slightly decreased density as optic chiasm for 3 to 4 mm, which corresponded to two to three slices based on slice thickness used in the current study.

3.3.2 Statistical Analysis

For each image set, the TPS was used to measure the Dice similarity coefficient (DSC) between each observer's optic pathway contour and the expert consensus contour.

The median, range, and 5^{th} and 95^{th} percentiles were calculated for the DSC before and after the training atlas intervention. A multilevel mixed model with random effects to account for repeated measures on patients and by observers was used to examine the difference in the DSC before and after the training atlas intervention; predicted mean differences between pre- and post-training were reported with 95% confidence intervals. The Kruskal-Wallis test was used to assess association between dog weight category ($>$ or $\leq$ the median weight) and the DSC for optic pathway contours. P-values ≤ 0.05 were considered significant. Data analysis was designed with

support from an analytic epidemiologist. All analysis completed with commercially available software (STATA/SE version 17 for Windows, StataCorp, College Station, TX).

3.4 Results

The median age and weight of the study dogs was 12.6 years (range, 11 to 15.3 years) and 23.5 kg (range, 11 to 53 kg), respectively. There were two neutered males, five spayed females, and one intact female. Breeds included mixed (n = 4), Dachshund (n = 1), Queensland Blue Heeler (n = 1), Border Collie (n = 1), and Newfoundland (n = 1). Six of the dogs were referred for treatment of an oral melanoma, and two were referred with nasal adenocarcinoma. One dog was brachycephalic while the remaining 7 were mesaticephalic. The median volume of the dogs' optic pathway contours reached by expert consensus was 1.25 cm^3 (range, 0.7 to 3 cm^3).

Invitations by email were sent to 114 board certified veterinary radiation oncologists, of which 36 agreed to participate. Of the 36 participants, 28 completed the first phase of contouring on all eight dogs, with 21 completing the second phase of contouring. Participants who failed to complete both phases of contouring were excluded from analysis (n = 7).

During the first phase of contouring, registration errors between the provided soft tissue and bone CT reconstructions were found in three dogs. The errors were small, and it was assumed that slight movement of the patient between successive scans that could not be accounted for in the TPS auto-registration was responsible for the error. After the registration errors were corrected, all participants were given the opportunity to review their contours for accuracy. One participant was unable to review their contours before the start of phase two, therefore the contours by that participant for these three dogs were excluded from analysis. It was also found that for one dog, the soft tissue reconstruction provided to participants was pre-

contrast. By the time this was noticed, the raw CT data had been deleted and it was not possible to generate a new reconstruction, so no correction was made.

Ninety-six percent (27/28) of respondents completed the online questionnaire. Participants who did not complete phase two contours were included in the questionnaire results because the survey was anonymous and therefore participants who did not complete phase two could not be identified. Responses to the questionnaire are presented in Table 3.1. Of the six respondents who indicated that the TPS used for the study prevented them from using their normal contouring practices, five commented that the transverse plane resolution did not allow for a small enough brush size, and one did not explain their answer. General comments on the study included more detailed information about optic nerve contouring at the participants' practice (n = 4).

The median DSC for the first phase of contouring, which was prior to training, was 0.31 (5^{th} and 95^{th} percentile, 0.06, 0.48). Phase two median DSC was 0.41 (5^{th} and 95^{th} percentile, 0.18, 0.53).

The mean DSC for the optic pathway contours was significantly higher after training than before training (mean difference = 0.10, 95% CI 0.08 to 0.12, $p < 0.001$) on average across all observers and patients. Dogs weighing ≤ 23.5 kg had a median DSC of 0.33 (5^{th} and 95^{th} percentile 0.1, 0.5), which was significantly ($p < 0.001$) lower than the median DSC of 0.41 (5^{th} and 95^{th} percentile 0.08, 0.53) for dogs weighing > 23.5 kg. Body weight and consensus optic pathway volume were highly correlated (correlation metric 0.93).

3.5 Discussion

Manual segmentation of the canine optic pathway was significantly improved following specific training guidelines implemented for use of the optic plane and window settings to optimize optic nerve and chiasm visualization.

While the optimal setting for individual systems may vary, the window level setting of 40 and width of 150 was found to provide the most contrast between soft tissue and the optic nerves on the test system used for the current study. It is important to note however, the window level setting must be applied to the standard or soft-tissue reconstructions. Modifications to the image data from other reconstruction algorithms remove image data in this viewing region that impairs visualization of the optic nerves.

The total number of slices to contour will vary based on slice thickness and transverse window size, although for the current study, six to ten slices in the optic plane was sufficient to contour the extracranial optic nerves for most of the dogs. While contouring in the optic plane, some bleed through of the contours to slices before and after the contoured slice will occur. This is presumably due to the non-spherical shape of the voxels making up the three-dimensional representation of the dog and it can make delineating the optic nerves more challenging in this plane. Additionally, the contours will become very small for one to three slices after switching back to the transverse view at the caudal end of the contour. This is due to the rounded end of the contour as it is translated back to a transverse view. These slices should be expanded to ensure they are at least 3 to 4 mm.

The accuracy of CT-based contours remained low after training, and DSC values were comparable to those reported for manual and automatic segmentation of the optic chiasm and nerves in human patients with a DSC range of 0.4 to 0.5. The study compared contours of eight

physicians to two auto-segmentation methods on twenty patients in which the eyes, optic pathway and brainstem were contoured.[14] The low DSC score can be explained by the small volume of the optic pathway. Because the DSC compares true positive, or the voxels included in both contours to the false negative and true negative, or the voxels contoured by only one contour, then if for both a large structure and a small structure the same number of voxels fall into the true or false negative category, the resulting ratio between positive and negative will be smaller and result in a lower DSC for the smaller structure. Our finding of lower accuracy in smaller dogs was consistent with the supposition that smaller volumes reduce DSC values. Other possible factors that may have negatively affected post-training accuracy may have been the use of low-quality monitors. If a participant contoured on a low-quality laptop screen using bony landmarks for contouring the optic pathway, the image quality would not be as impactful as when visualizing subtle attenuation changes between optic nerve and soft tissue. Minimum contouring brush sizes available in the TPS of 3 mm (n= 2), 4 mm (n = 3), or 5 mm (n = 1) for some dogs could have resulted in inferior contours in either phase due to the increased difficulty in contouring smaller volumes. This limitation was presumably due to a combination of both the small patient size and increased dimensions of the transverse window of the image. With six participants stating that they never contour the optic pathway on CT, and one stating that they have not done any contouring over the past two years, lack of contouring experience could also be a reason for reduced accuracy in both phases, however we do not know if these six participants completed both phases of contouring. The training method could have negatively impacted phase two accuracy also. The instructions may have been unclear or difficult to understand, and it is also possible that participants failed to use the training atlas and video as instructed.

Even though participants contoured three separate structures, the decision was made to present results for the entire optic pathway (combined optic nerves and chiasm) because a small number of participants mixed the left and right optic nerves and there was a subset of participants that contoured the optic nerves within the optic canal as chiasm in phase one (n = 6). Despite instructions in the training atlas for how to contour the optic chiasm, some participants continued to contour chiasm into the optic canal in phase two (n = 3). The instructions for contouring the optic chiasm in the training atlas were developed to be consistent with the published anatomical description, which states that the chiasm is caudal to the optic canal at the rostroventral floor of the middle cranial fossa, where the fibers from the left and right optic nerve cross.[15] Combining all structures into a single contour eliminated participant variability for when the optic nerves end and the chiasm begins.

Accurate contouring of each portion of the optic pathway separately can aid in treatment planning; however, if one eye must be sacrificed to adequately treat a tumor, it may be possible to spare vision in the contralateral eye. In such an instance, it would be important to keep dose below the tolerance level in one optic nerve and the chiasm and separate structures for the left and right optic nerves may be desirable.

Recommended brush size of this study of 3mm to 4mm matches closely with measurements performed previously. One study found a mean diameter of 3.7 mm for the optic nerve sheath for a similar group of dogs that were somewhat smaller (mean 17.0 Kg) comprised of five crossbreeds, four Beagles, and one Labrador Retriever. This study also utilized a dorsal oblique (optic plane) MRI scanning angle and distinguished between the optic nerve and optic nerve sheath.[12] The current study chose not to distinguish between optic nerve and optic nerve sheath because it is not possible to make that distinction on CT imaging.

To the authors knowledge, there is not another study investigating accuracy of contours drawn on non-standard viewing planes. Prior recommendations have been to draw contours on the transverse view, with Scoccianti recommending observation of positioning in the dorsal and sagittal views to verify location.[10,16]

This study has shown that it is possible to reliably distinguish nerves from surrounding soft tissue when appropriate windowing and viewing angle are selected. It may be possible to apply this technique to nerves near other sites treated with radiation therapy, to more accurately apply constraints.

Future studies investigating alternative contouring methods may benefit from a live hands-on training session so that participants can ask questions and receive feedback. Multiple presentation formats would better support multiple learning styles and ensure better compliance with the technique. Additional research could also be performed to investigate optic nerve movements over successive anesthetic events. Costa found that the anesthetic protocol can affect globe position[17] and Drolet uncovered ultrasonographic evidence that optic nerve sheath diameter is impacted by anesthesia.[18] Research into optic nerve movement could result in the recommendation for an expansion on delineation to allow for movement.

Contours created in the optic plane will in many instances translate to contours in the transverse plane that are not smooth. The impact on the TPS of this characteristic was not explored, however it is presumably dependent on the implementation of the dose calculation algorithm and readers who create contours in the optic plane should contact the software development team for their TPS for guidance on the need to smooth contours in the transverse or other plane for OARs.

One important limitation of this study is the small number of brachycephalic dogs. The recruitment period available for this study was limited, and only one brachycephalic dog was

presented for radiation during the period. Consequently, results from this study may not be applicable to brachycephalic dogs. The brachycephalic dog in this study had the lowest average scores from both phases, however it was also the smallest dog by weight. Another limitation was the limited MRI sequences available for the expert reference contours. In order to meet imaging time constraints at this institution, some cases only had the optic plane T2 fat saturation sequence covering the optic pathway.

Use of MR imaging for optic pathway contouring is expected to provide the highest accuracy, especially with low body weight dogs; however, when CT alone is used, our study supports routine use of an optic plane contouring method as described above with window level of 40 and a window width of 150 to improve segmentation accuracy.

Table 3.1. Optic pathway contouring practices of members of the American College of Veterinary Radiology (Subspecialty Radiation Oncology) (n = 27 respondents).

Variable		**N**	**%**
Which statement best describes how frequently, on average, contouring of the optic pathway on CT is part of your clinical practice?	≥ one CT optic pathway contouring per day	2	7
	< one CT per day, ≥ one CT optic pathway contouring per week	8	30
	< one CT per week, ≥ one CT optic pathway contouring per month	6	22
	< one CT optic pathway contouring per month	5	19
	Never contour optic pathway on CT images	6	22
Which plane(s) of CT imaging do you use for contouring the optic pathway?[a]	Transverse (axial)	24	96
	Dorsal (frontal)	22	88
	Sagittal	17	68
	Other	8	29
For approximately what percentage of optic pathway contouring do you use those CT plane(s)?[b]	Transverse (axial)		68
	Dorsal (frontal)		22
	Sagittal		6
	Other		4
Did the study treatment planning software prevent you	Yes	6	22
	No	21	78

from performing any of your normal contouring practices?			
At what type of practice do you primarily work?	Academia Private practice Other	18 8 1	67 30 4

[a]Twenty-five participants answered this question

[b]The percentage of time the plane was used across all participants

Figure 3.1 List of steps for contouring the optic pathway.

1. Use a window level of 40 and a window width of 150 (corresponding to an upper grey level of 115 and a lower grey level of -35).
2. Rotate the sagittal view until the hard palate of the dog is approximately 35 to 45 degrees off the vertical axis.
3. Use the dorsal plane window, now the optic plane, to make slight adjustments to the viewing angle to maximize the length of visible nerve.
4. Contour the optic nerves from the caudal globe to the opening of the optic canal.
5. Use the transverse view and bone windowing to extend the optic nerve contours caudally through the optic canal to the level at which the presphenoid bone between the two canals begins to recede.
6. Starting on the next slice caudally, switch back to a window level of 40 and a window width of 150 and contour the region of slightly decreased density as optic chiasm for 2-3 slices.

Figure 3.2 Canine image at the angle of the optic plane in MR (a) and CT (b). White arrows point to the optic nerves.

a) b)

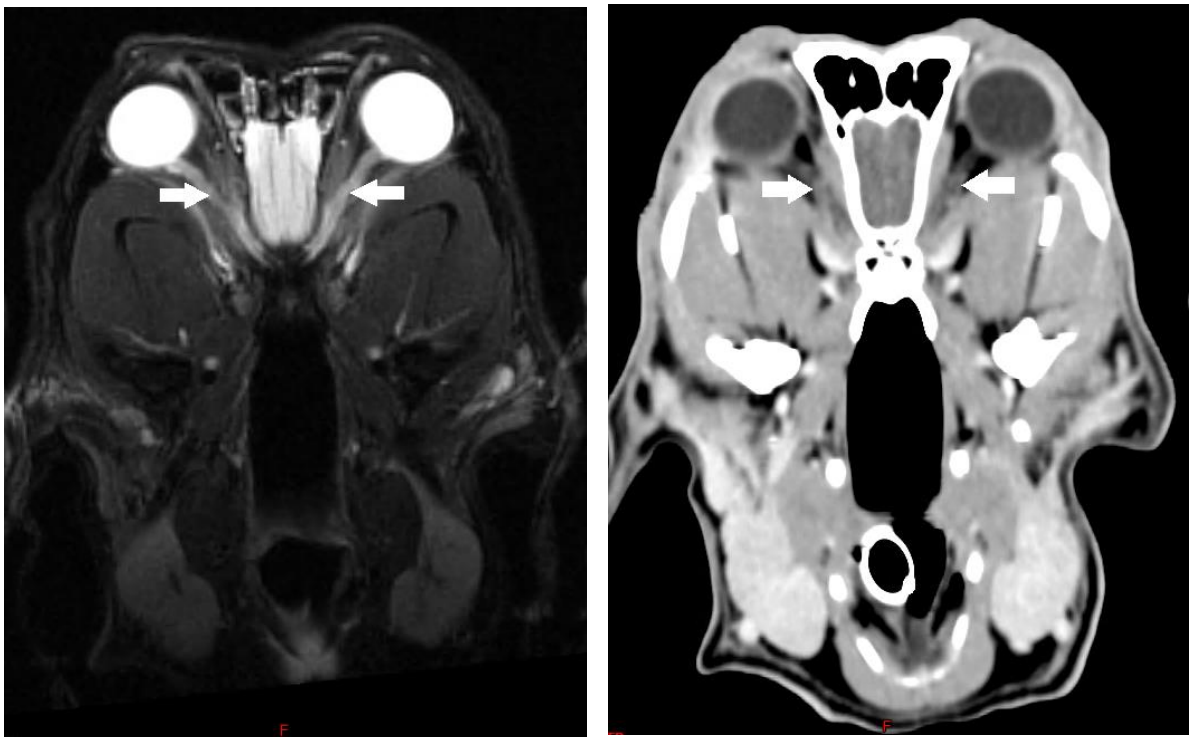

4. Chapter Four: Conclusion

Segmentation inconsistencies demonstrated in both studies presented highlight a deficiency in veterinary radiation oncology. Both a lack of adequate imaging, as outlined in the dosimetry study and improper contouring technique, outlined in the optic pathway study highlight contributing causes to this deficiency. Consequences of the variations in contouring have a wide-ranging impact, from the individual patient not gaining adequate tumor control or suffering from an avoidable late toxicity, to research, where outcomes could be as dependent on contouring variations as much as treatment prescriptions. As a profession, it will be important to work towards reducing the highlighted inconsistencies to improve both individual patient outcome and enable research to make more reliable progress.

A number of steps could be taken to improve segmentation consistency and accuracy. Formal contouring training could be incorporated into residency programs to ensure that all future veterinary radiation oncologists employ proper contouring techniques. Veterinary contouring guidelines could also be established to provide a framework for best contouring practices. Another step that could be taken to reduce contouring variations and improve accuracy is the implementation of group case reviews. Auto-segmentation is an as-yet unexplored enhancement in veterinary medicine that could be a benefit to patients. And finally, increased availability of MRI and PET/CT would help reduce uncertainty and variability in veterinary contouring.

References

For Chapter 2:

1. Kishimoto TE, Uchida K, Chambers JK, Kok MK, Son NV, Shiga T, Hirabayashi M, Ushio N, Nakayama H. A retrospective survey on canine intracranial tumors between 2007 and 2017. J Vet Med Sci. 2020 Jan 17;82(1):77-83.

2. Snyder JM, Shofer FS, Van Winkle TJ, Massicotte C. Canine intracranial primary neoplasia: 173 cases (1986-2003). J Vet Intern Med. 2006 May-Jun;20(3):669-75.

3. Sudhyadhom A. On the molecular relationship between Hounsfield Unit (HU), mass density, and electron density in computed tomography (CT). PLoS One. 2020 Dec 31;15(12):e0244861.

4. Drees R, Forrest LJ, Chappell R. Comparison of computed tomography and magnetic resonance imaging for the evaluation of canine intranasal neoplasia. J Small Anim Pract. 2009 Jul;50(7):334-40.

5. Kupelian P, Sonke JJ. Magnetic resonance-guided adaptive radiotherapy: a solution to the future. Semin Radiat Oncol. 2014 Jul;24(3):227-32.

6. Khoo VS, Adams EJ, Saran F, Bedford JL, Perks JR, Warrington AP, Brada M. A Comparison of clinical target volumes determined by CT and MRI for the radiotherapy planning of base of skull meningiomas. Int J Radiat Oncol Biol Phys. 2000 Mar 15;46(5):1309-17.

7. Griffin LR, Nolan MW, Selmic LE, Randall E, Custis J, LaRue S. Stereotactic radiation therapy for treatment of canine intracranial meningiomas. Vet Comp Oncol. 2016 Dec;14(4):e158-e170.

8. Mariani CL, Schubert TA, House RA, Wong MA, Hopkins AL, Barnes Heller HL, Milner RJ, Lester NV, Lurie DM, Rajon DA, Friedman WA, Bova FJ. Frameless stereotactic radiosurgery for the treatment of primary intracranial tumours in dogs. Vet Comp Oncol. 2015 Dec;13(4):409-23.

9. Keyerleber MA, McEntee MC, Farrelly J, Thompson MS, Scrivani PV, Dewey CW. Three-dimensional conformal radiation therapy alone or in combination with surgery for treatment of canine intracranial meningiomas. Vet Comp Oncol. 2015 Dec;13(4):385-97.

10. Weltens C, Menten J, Feron M, Bellon E, Demaerel P, Maes F, Van den Bogaert W, van der Schueren E. Interobserver variations in gross tumor volume delineation of brain tumors on computed tomography and impact of magnetic resonance imaging. Radiother Oncol. 2001 Jul;60(1):49-59.

11. Hartgerink D, Swinnen A, Roberge D, Nichol A, Zygmanski P, Yin FF, Deblois F, Hurkmans C, Ong CL, Bruynzeel A, Aizer A, Fiveash J, Kirckpatrick J, Guckenberger M, Andratschke N, de Ruysscher D, Popple R, Zindler J. LINAC based stereotactic radiosurgery for multiple brain metastases: guidance for clinical implementation. Acta Oncol. 2019 Sep;58(9):1275-1282.

12. Morimoto CY, Waldner CL, Fan V, Sidhu N, Matthews Q, Randall E, Griffin L, Keyerleber M, Rancilio N, Vanhaezebrouck I, Zwueste D, Mayer MN. Use of MRI increases interobserver agreement on gross tumor volume for imaging-diagnosed canine intracranial meningioma. Vet Radiol Ultrasound. 2020 Oct 8. doi: 10.1111/vru.12915.

13. Hellebust TP, Tanderup K, Lervåg C, Fidarova E, Berger D, Malinen E, Pötter R, Petrič P. Dosimetric impact of interobserver variability in MRI-based delineation for cervical cancer brachytherapy. Radiother Oncol. 2013 Apr;107(1):13-9.

14. Batumalai V, Burke S, Roach D, Lim K, Dinsdale G, Jameson M, Ochoa C, Veera J, Holloway L, Vinod S. Impact of dosimetric differences between CT and MRI derived target volumes for external beam cervical cancer radiotherapy. Br J Radiol. 2020 Oct 1;93(1114):20190564.

15. Berry SL, Boczkowski A, Ma R, Mechalakos J, Hunt M. Interobserver variability in radiation therapy plan output: Results of a single-institution study. Pract Radiat Oncol. 2016 Nov-Dec;6(6):442-449.

16. Warfield SK, Zou KH, Wells WM. Simultaneous truth and performance level estimation (STAPLE): an algorithm for the validation of image segmentation. IEEE Trans Med Imaging. 2004 Jul;23(7):903-21.

17. Folkert MR, Timmerman RD. Stereotactic ablative body radiosurgery (SABR) or Stereotactic body radiation therapy (SBRT). Adv Drug Deliv Rev. 2017 Jan 15;109:3-14.

18. Paddick I. A simple scoring ratio to index the conformity of radiosurgical treatment plans. Technical note. J Neurosurg. 2000 Dec;93 Suppl 3:219-22.

19. Shaw E, Kline R, Gillin M, Souhami L, Hirschfeld A, Dinapoli R, Martin L. Radiation Therapy Oncology Group: radiosurgery quality assurance guidelines. Int J Radiat Oncol Biol Phys. 1993 Dec 1;27(5):1231-9.

20. Bekelman JE, Wolden S, Lee N. Head-and-neck target delineation among radiation oncology residents after a teaching intervention: a prospective, blinded pilot study. Int J Radiat Oncol Biol Phys. 2009 Feb 1;73(2):416-23.

21. Konert T, Vogel WV, Everitt S, MacManus MP, Thorwarth D, Fidarova E, Paez D, Sonke JJ, Hanna GG. Multiple training interventions significantly improve reproducibility of PET/CT-

based lung cancer radiotherapy target volume delineation using an IAEA study protocol. Radiother Oncol. 2016 Oct;121(1):39-45.

22. Onal C, Cengiz M, Guler OC, Dolek Y, Ozkok S. The role of delineation education programs for improving interobserver variability in target volume delineation in gastric cancer. Br J Radiol. 2017 May;90(1073):20160826.

23. Mercieca S, Belderbos JSA, van Baardwijk A, Delorme S, van Herk M. The impact of training and professional collaboration on the interobserver variation of lung cancer delineations: a multi-institutional study. Acta Oncol. 2019 Feb;58(2):200-208.

24. Hussain STA, Rapole PS, Sethi P, Veluthattil AC, Patil N, Ramalingam C, Thulasingam M. Target Volume Delineation Training in Radiation Oncology in India : A Survey Evaluating Its Status, the Need for Educational Programs and the Utility of Virtual Teaching. Asian Pac J Cancer Prev. 2021 Dec 1;22(12):3875-3882.

25. Prins FM, van der Velden JM, Gerlich AS, Kotte ANTJ, Eppinga WSC, Kasperts N, Verlaan JJ, Pameijer FA, Kerkmeijer LGW. Superior target delineation for stereotactic body radiotherapy of bone metastases from renal cell carcinoma on MRI compared to CT. Ann Palliat Med. 2017 Dec;6(Suppl 2):S147-S154.

26. Piazzese C, Evans E, Thomas B, Staffurth J, Gwynne S, Spezi E. FIELD^{RT}: an open-source platform for the assessment of target volume delineation in radiation therapy. Br J Radiol. 2021 Oct 1;94(1126):20210356.

27. Stanley J, Dunscombe P, Lau H, Burns P, Lim G, Liu HW, Nordal R, Starreveld Y, Valev B, Voroney JP, Spencer DP. The effect of contouring variability on dosimetric parameters for brain metastases treated with stereotactic radiosurgery. Int J Radiat Oncol Biol Phys. 2013 Dec 1;87(5):924-31.

28. SandstrÖm H, Toma-Dasu I, Chung C, GÅrding J, Jokura H, Dasu A. Simultaneous Truth and Performance Level Estimation Method for Evaluation of Target Contouring in Radiosurgery. Anticancer Res. 2021 Jan;41(1):279-288.

29. Redmond KJ, Robertson S, Lo SS, Soltys SG, Ryu S, McNutt T, Chao ST, Yamada Y, Ghia A, Chang EL, Sheehan J, Sahgal A. Consensus Contouring Guidelines for Postoperative Stereotactic Body Radiation Therapy for Metastatic Solid Tumor Malignancies to the Spine. Int J Radiat Oncol Biol Phys. 2017 Jan 1;97(1):64-74.

30. Cox BW, Spratt DE, Lovelock M, Bilsky MH, Lis E, Ryu S, Sheehan J, Gerszten PC, Chang E, Gibbs I, Soltys S, Sahgal A, Deasy J, Flickinger J, Quader M, Mindea S, Yamada Y. International Spine Radiosurgery Consortium consensus guidelines for target volume definition in spinal stereotactic radiosurgery. Int J Radiat Oncol Biol Phys. 2012 Aug 1;83(5):e597-605.

31. Lim K, Small W Jr, Portelance L, Creutzberg C, Jürgenliemk-Schulz IM, Mundt A, Mell LK, Mayr N, Viswanathan A, Jhingran A, Erickson B, De los Santos J, Gaffney D, Yashar C, Beriwal S, Wolfson A, Taylor A, Bosch W, El Naqa I, Fyles A; Gyn IMRT Consortium. Consensus guidelines for delineation of clinical target volume for intensity-modulated pelvic radiotherapy for the definitive treatment of cervix cancer. Int J Radiat Oncol Biol Phys. 2011 Feb 1;79(2):348-55.

32. Soliman H, Ruschin M, Angelov L, Brown PD, Chiang VLS, Kirkpatrick JP, Lo SS, Mahajan A, Oh KS, Sheehan JP, Soltys SG, Sahgal A. Consensus Contouring Guidelines for Postoperative Completely Resected Cavity Stereotactic Radiosurgery for Brain Metastases. Int J Radiat Oncol Biol Phys. 2018 Feb 1;100(2):436-442.

33. Dunne EM, Sahgal A, Lo SS, Bergman A, Kosztyla R, Dea N, Chang EL, Chang UK, Chao ST, Faruqi S, Ghia AJ, Redmond KJ, Soltys SG, Liu MC. International consensus recommendations for target volume delineation specific to sacral metastases and spinal stereotactic body radiation therapy (SBRT). Radiother Oncol. 2020 Apr;145:21-29.

For Chapter 3:

1. Griffin LR, Nolan MW, Selmic LE, Randall E, Custis J, LaRue S. Stereotactic radiation therapy for treatment of canine intracranial meningiomas. Vet Comp Oncol. 2016 Dec;14(4):e158-e170.

2. Kelsey KL, Gieger TL, Nolan MW. Single fraction stereotactic radiation therapy (stereotactic radiosurgery) is a feasible method for treating intracranial meningiomas in dogs. Vet Radiol Ultrasound. 2018 Sep;59(5):632-638.

3. Dolera M, Malfassi L, Pavesi S, Marcarini S, Sala M, Mazza G, Carrara N, Finesso S, Urso G. Stereotactic Volume Modulated Arc Radiotherapy in Canine Meningiomas: Imaging-Based and Clinical Neurological Posttreatment Evaluation. J Am Anim Hosp Assoc. 2018 Mar/Apr;54(2):77-84.

4. Fox-Alvarez S, Shiomitsu K, Lejeune AT, Szivek A, Kubicek L. Outcome of intensity-modulated radiation therapy-based stereotactic radiation therapy for treatment of canine nasal carcinomas. Vet Radiol Ultrasound. 2020 May;61(3):370-378.

5. Gieger TL, Nolan MW. Linac-based stereotactic radiation therapy for canine non-lymphomatous nasal tumours: 29 cases (2013-2016). Vet Comp Oncol. 2018 Mar;16(1):E68-E75.

6. Reczynska AI, LaRue SM, Boss MK, Lee BI, Leary D, Pohlmann K, Griffin L, Lana S, Wormhoudt Martin T. Outcome of stereotactic body radiation for treatment of nasal and nasopharyngeal lymphoma in 32 cats. J Vet Intern Med. 2022 Mar;36(2):733-742.

7. Benedict SH, Yenice KM, Followill D, Galvin JM, Hinson W, Kavanagh B, Keall P, Lovelock M, Meeks S, Papiez L, Purdie T, Sadagopan R, Schell MC, Salter B, Schlesinger DJ, Shiu AS, Solberg T, Song DY, Stieber V, Timmerman R, Tomé WA, Verellen D, Wang L, Yin FF. Stereotactic body radiation therapy: the report of AAPM Task Group 101. Med Phys. 2010 Aug;37(8):4078-101.

8. Folkert MR, Timmerman RD. Stereotactic ablative body radiosurgery (SABR) or Stereotactic body radiation therapy (SBRT). Adv Drug Deliv Rev. 2017 Jan 15;109:3-14.

9. Timmerman R. A Story of Hypofractionation and the Table on the Wall. Int J Radiat Oncol Biol Phys. 2022 Jan 1;112(1):4-21.

10. Nolan MW, Randall EK, LaRue SM, Lunn KF, Stewart J, Kraft SL. Accuracy of CT and MRI for contouring the feline optic apparatus for radiation therapy planning. Vet Radiol Ultrasound. 2013 Sep-Oct;54(5):560-6.

11. Parry AT, Volk HA. Imaging the cranial nerves. Vet Radiol Ultrasound. 2011 Mar-Apr;52(1 Suppl 1):S32-41.

12. Boroffka SA, Görig C, Auriemma E, Passon-Vastenburg MH, Voorhout G, Barthez PY. Magnetic resonance imaging of the canine optic nerve. Vet Radiol Ultrasound. 2008 Nov-Dec;49(6):540-4.

13. Andrews EF, Jacqmot O, Espinheira Gomes FNCM, Sha MF, Niogi SN, Johnson PJ. Characterizing the canine and feline optic pathways in vivo with diffusion MRI. Vet Ophthalmol. 2021 Nov 16.

14. Deeley MA, Chen A, Datteri R, Noble JH, Cmelak AJ, Donnelly EF, Malcolm AW, Moretti L, Jaboin J, Niermann K, Yang ES, Yu DS, Yei F, Koyama T, Ding GX, Dawant BM. Comparison of manual and automatic segmentation methods for brain structures in the presence of space-occupying lesions: a multi-expert study. Phys Med Biol. 2011 Jul 21;56(14):4557-77.

15. Hermanson, J. W., Miller, M. E., DeLahunta, A., & Evans, H. E. (2020). Miller and Evans' anatomy of the dog (Fifth). Elsevier.

16. Scoccianti S, Detti B, Gadda D, Greto D, Furfaro I, Meacci F, Simontacchi G, Di Brina L, Bonomo P, Giacomelli I, Meattini I, Mangoni M, Cappelli S, Cassani S, Talamonti C, Bordi L,

Livi L. Organs at risk in the brain and their dose-constraints in adults and in children: a radiation oncologist's guide for delineation in everyday practice. Radiother Oncol. 2015 Feb;114(2):230-8.

17. Costa D, Leiva M, Moll X, Aguilar A, Peña T, Andaluz A. Alfaxalone versus propofol in dogs: a randomised trial to assess effects on peri-induction tear production, intraocular pressure and globe position. Vet Rec. 2015 Jan 17;176(3):73.

18. Drolet C, Pinard C, Gaitero L, Monteith G, Bateman S. Study of the effect of anaesthesia on the canine ultrasonographic optic nerve sheath diameter. J Small Anim Pract. 2021 Dec;62(12):1070-1078.